PHOTOELECTRON SPECTROSCOPY OF HI AND PHOTOEMISSION FOLLOWING NARROWBAND VUV EXCITATION

N. Böwering, T. Huth, A. Mank, M. Müller, G. Schönhense, R. Wallenstein, and U. Heinzmann

Universität Bielefeld, Fakultät für Physik
D-4800 Bielefeld, West-Germany
and Fritz-Haber-Institut der MPG
D-1000 Berlin 33, West-Germany

INTRODUCTION

As a model case for a detailed photoelectron spectroscopy of molecules, the photoelectron emission of hydrogen iodide was studied. The experiments were performed in the autoionization region between the $HI^+ {}^2\Pi_{3/2}$ and $^2\Pi_{1/2}$ thresholds and between the $HI^+ {}^2\Pi_{1/2}$ and $^2\Sigma^+$ thresholds. For the region between the $HI^+ {}^2\Pi$ thresholds where the autoionization features are sharp, a novel scheme for very high resolution photoelectron yield measurements was applied using laser frequency upconversion to the vacuum ultraviolet (VUV).[1] The system is capable to produce rotationally resolved spectra. At photon energies above the $^2\Pi$ limits where the ionization structures are much broader, synchrotron radiation at the Berlin storage ring BESSY was used for angle-resolved photoelectron spectroscopy and measurements of the photoelectron spin polarization[2]. With this apparatus, vibrational excitation in the final states was detected and the energy dependence of the dynamical photoionization parameters was determined.

HIGH RESOLUTION YIELD MEASUREMENTS

For narrow-band excitation, VUV radiation is generated by resonantly enhanced sum-frequency mixing of two pulsed dye lasers in mercury vapor.[3] Both dye lasers are pumped by Nd:YAG lasers. Dye laser 1 is frequency doubled to produce ultraviolet (UV) radiation at λ = 280.3 nm (pulse energy 8 mJ) for excitation of the Hg 6^1S - 6^1D two-photon resonance. Dye laser 2 (5 mJ) is tuned in the wavelength range of λ = 600 - 730 nm. Thus, coherent VUV radiation is generated in the range of λ = 113.5 - 117.5 nm in a mixing process which is very efficient due to its two-photon resonant character.

The experimental set-up is shown schematically in Fig. 1. The two synchronized dye-laser beams are combined with a dichroic mirror, and are focussed with matched foci into a heat pipe containing mercury at p = 1.5 mbar and neon at p = 4 mbar. The sum-frequency radiation generated enters the vacuum system through a lithium fluoride (LiF) window and is separated from other UV and VUV radiation by means of a LiF-prism

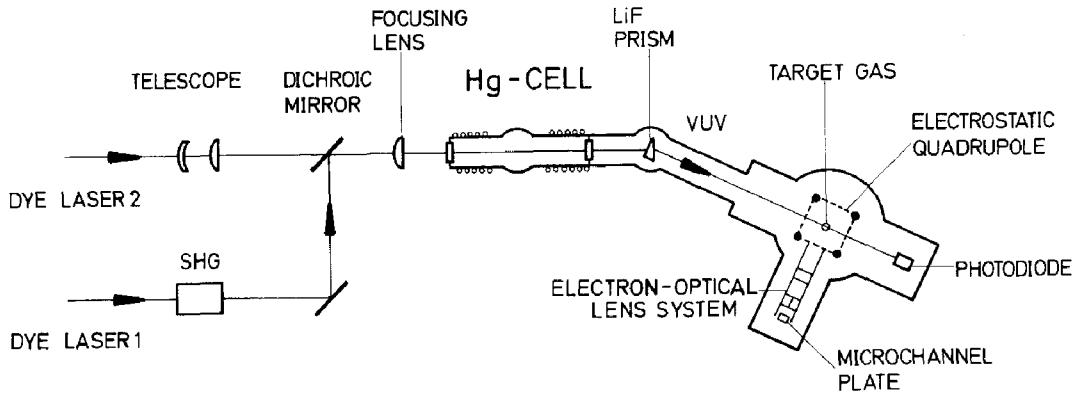

Fig. 1: Experimental apparatus for resonant sum frequency mixing and photoionization yield spectroscopy.

and beam dumps. Typically, 10^{10} photons per pulse (about 3 ns FWHM) are produced at a repetition rate of 10 Hz. The spectral resolution as determined by the bandwidth of the visible laser radiation is calculated to be 4.5×10^{-4} nm.

In the excitation region the VUV light is crossed at right angles by a focussed beam of HI molecules generated by a bent capillary plate used as nozzle. The photoelectrons produced are collected by a quadrupole

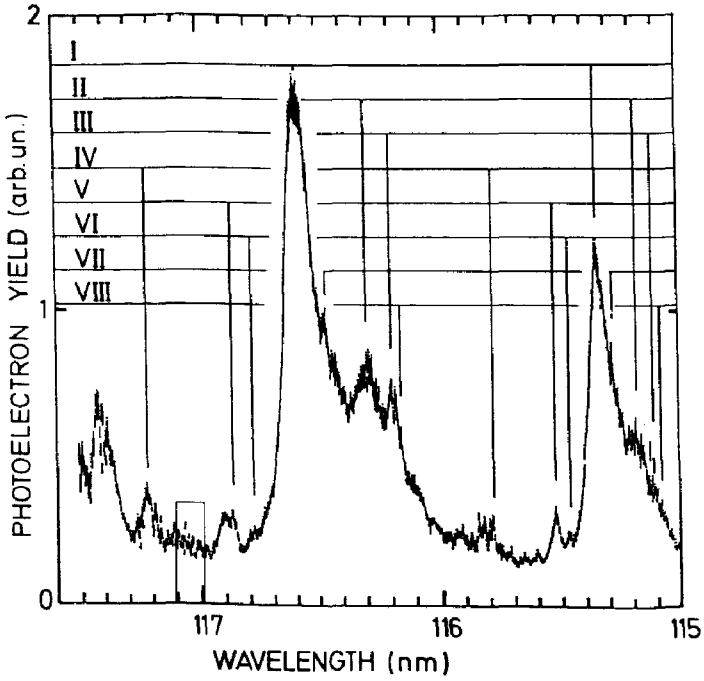

Fig. 2: Coarse scan through n = 6, 7 members of the $HI^+ {}^2\Pi$ autoionization region. Data points are drawn as vertical lines to denote the experimental uncertainty. Extending the assignments of Ref. 4, several Rydberg series are identified and labelled in the figure.

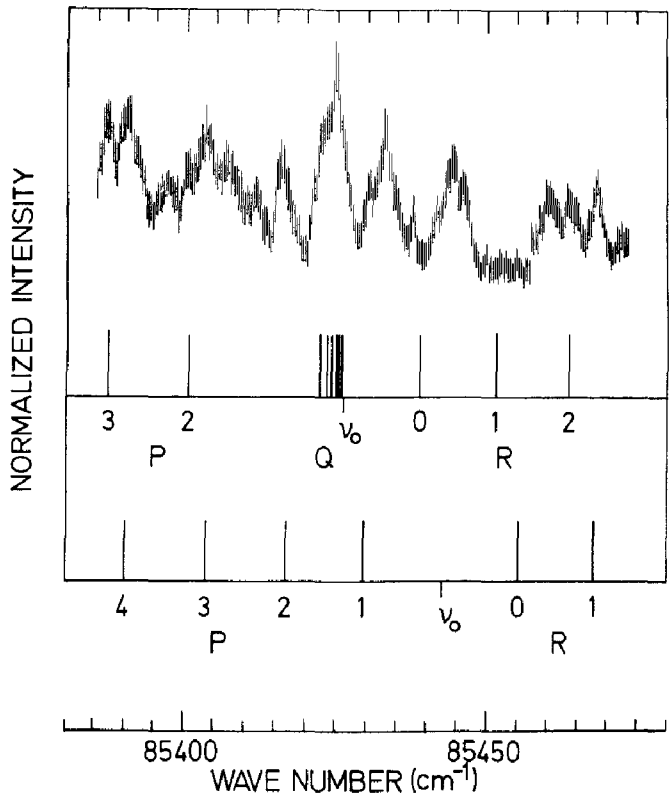

Fig. 3: High resolution scan through the structures around 117 nm (indicated by box in Fig. 2). Step size is 4.5×10^{-4} nm. A tentative assignment of possible rotational fine structure for two transitions is indicated in the lower part of the figure.

field and an electron-optical lens system and detected with a microchannel plate. The photoelectron signal is normalized to the VUV intensity as measured with a vacuum photodiode; each spectral sample is averaged over 20 to 100 laser shots and each scan is repeated several times.

Fig. 2 shows a broad scan with coarse step size of 3×10^{-3} nm over the range of λ = 115 to 117.5 nm. The envelope of the data compares well with the results from photoionization mass spectrometry of Eland and Berkowitz[4] taken at a resolution of 7×10^{-3} nm. The assignment of the Rydberg series by these authors was guided by the analogy to xenon which is the united atom limit of HI. Classification of the main resonances can be accomplished by comparison with the recent theoretical MQDT calculation for n = 6 of Lefebvre-Brion et al.[5]. However, the highly resolved spectra reveal a rich underlying structure which can only be attributed to a small extend to series converging to vibrationally excited levels and is probably largely due to the influence of rotational structure. Additional features may result from L- and S-uncoupling effects[5].

For broad resonances like series I, broadening of the line profiles due to the short lifetime of the autoionizing state dominates and should preclude any identification of rotational bands. Therefore, regions of the spectrum which contain weak but sharp resonances and low background levels were scanned with small step size in order to attempt an analysis of rotational substructure. Fig. 3 shows such a section obtained with

high resolution on an expanded scale. The peaks shown were reproducible in shape and intensity at equivalent conditions of the molecular beam. (The rotational temperature is estimated to lie in the range of 100 - 200 K.) Also drawn are rotational branches for two electronic transitions neglecting all broadening and assuming that the rotational constant of the upper state is 1.5% smaller than for the ground state of HI. The spectra are matched at a possible position of a Q-branch. It is clear from the spacing of the peaks observed that several spectral features overlap in this region and the assignment is not unique. Tentatively, a resonance with $\Omega = 1$ at 85426 cm^{-1} and a state with $\Omega = 0$ at 85442.5 cm^{-1} are identified.

VIBRATIONALLY RESOLVED PHOTOELECTRON SPECTROSCOPY

For energy-, angle- and spin-resolved photoelectron spectroscopy circularly polarized synchrotron radiation emitted out of plane at BESSY was used. At the exit focus of a normal incidence monochromator ($\Delta\lambda$ = 0.5 nm) the photoemission of HI from an effusive molecular beam is recorded. The photoionization cell is mounted on a liquid nitrogen cold trap and the background pressure inside the vacuum chamber is less than 9×10^{-5} mbar. The photoelectrons emitted in the reaction plane at a definite angle θ are energy-analyzed by a rotatable hemispherical spectrometer. Intensity spectra are recorded by a channeltron. For spin analysis, the electrons are accelerated to 100 keV and the two transverse electron spin-polarization components are measured with a Mott detector. A detailed description of the apparatus is given in Ref. 6.

Photoelectron spectra were taken at the magic angle ($\theta_m = 54.5°$) above the $HI^+ \ ^2\Pi$ thresholds with a resolution of $\Delta E \sim 120$ meV. Previously, no vibrational excitation higher than v = 1 was observed in the final ionic $^2\Pi$ states (which correspond to the removal of an electron from a nonbonding orbital) in photoelectron spectra taken with the He I resonance line[7,8], and in the range between the $HI^+ \ ^2\Pi_{3/2}$ and $^2\Pi_{1/2}$ limits[9]. Apparently, levels with v > 1 lie outside the Franck-Condon region. At photon energies above 13.5 eV levels with v > 1 were not found in this work, also, and the relative intensity of the (v = 1) levels was very low, in agreement with the He I spectrum of Ref. 8 (where I(v = 1) / I(v = 0) = 1/30). However, when tuned to the range above the $HI^+ \ ^2\Pi_{1/2}$ threshold and below the dissociation limit of HI^+ clear evidence of strong contributions of higher vibrationally excited states of both $^2\Pi_{1/2}$ and $^2\Pi_{3/2}$ is found as shown in Fig. 4. In this region, the vibrational branching changes drastically and vibrational levels of $HI^+ \ ^2\Pi_{1/2}$ up to v = 8 were detected at λ = 92.5 nm. The enhancement of higher vibrational excitation in the final ionic state is attributed to autoionizing Rydberg states converging to $HI^+ \ ^2\Sigma^+$. These states are excited in high vibrational levels and can decay with a large overlap to vibrationally excited levels of $HI^+ \ ^2\Pi$.

The relevant potential curves are shown in Fig. 5. The Rydberg states (labelled Ry in the figure) have a larger equilibrium internuclear separation since an electron of the more tightly bound 5pσ-orbital is excited. Lempka et al.[8] concluded from their He I photoelectron spectra and by comparison with the lighter hydrogen halides that due to the position of the curve crossing of the $HI^+ \ ^2\Sigma^+$ potential curve with the $^2\Pi$ repulsive curves all vibrational levels of $HI^+ \ ^2\Sigma^+$ are predissociating. Thus, the corresponding Rydberg states can be expected to be strongly predissociating, as well. Consistent with this picture, data from photoabsorption spectroscopy[10] and photoionization mass spectrometry[11] in this spectral region do not show distinct vibrational progressions of Rydberg series. Nevertheless, as demonstrated here, the vibrational

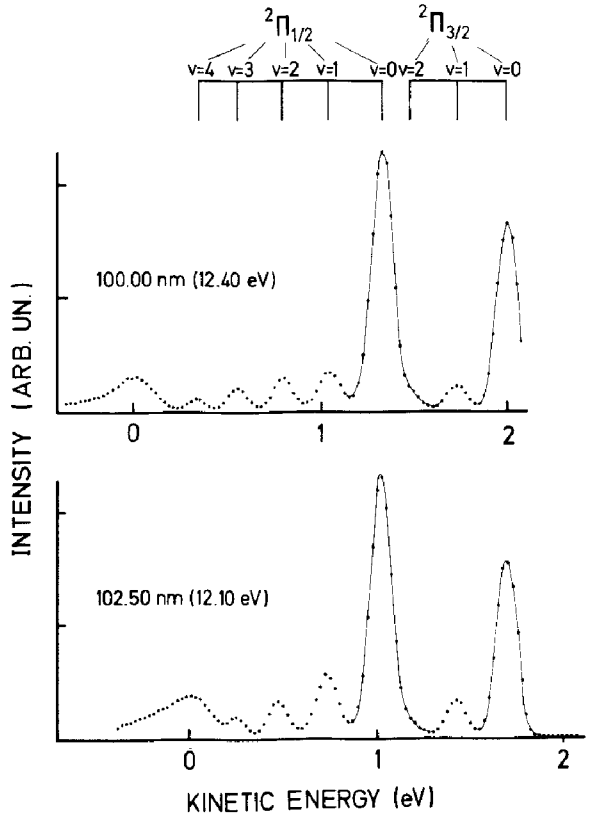

Fig. 4: Photoelectron spectra resolving vibrational excitation of the final $^2\Pi$-ionic states.
(The peak at 0 eV corresponds to a background of slow electrons.)

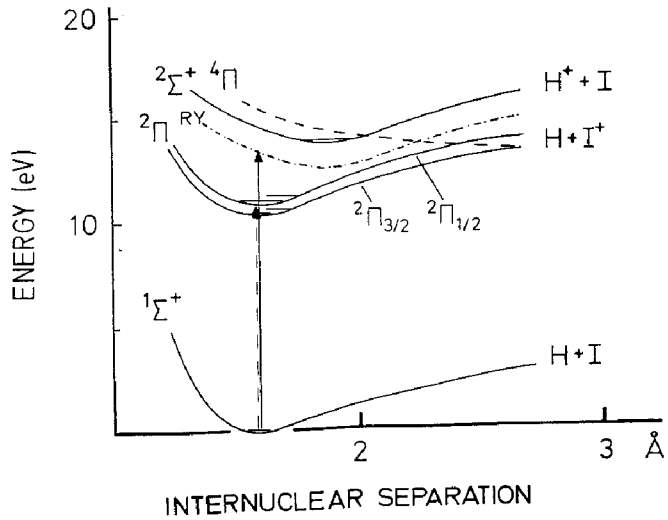

Fig. 5: Potential energy curves of HI. (Adapted from Ref. 8.) Indicated is excitation in the autoionization regions between the $^2\Pi$ states and between $^2\Pi$ and $^2\Sigma^+$.

excitation can be detected in the photoelectron spectra which reflect the vibrational excitation of the intermediate Rydberg state in the distribution for the final ionic states.

There is considerably less information on the ionic ground states for HI than for the lighter hydrogen halides. Spectra of the type of Fig. 4 were analysed to obtain information about vibrational frequencies. The centroids of the vibrational peaks were determined by assuming symmetric Gaussian distributions and the first differences of successive levels, $\Delta G_{v+1/2} = \omega_e - 2\omega_e x_e(v+1)$, were plotted against (v+1) to obtain the vibrational frequency $\omega_e = (2203 \pm 18)cm^{-1}$ and the anharmonicity constant $\omega_e x_e = (41.5 \pm 4.8)cm^{-1}$ for the $HI^+ \, ^2\Pi_{1/2}$ state. Since the series of $HI^+ \, ^2\Pi_{3/2}$ is "buried" under the peaks of $HI^+ \, ^2\Pi_{3/2}$, only the first differences $\Delta G_{1/2} = (2157 \pm 10)cm^{-1}$ and $\Delta G_{3/2} = (1920 \pm 26)cm^{-1}$ could be determined.

PHOTOELECTRON-SPIN POLARIZATION

The spin-polarization parameters A (characterizing the component $A(\theta)$ of the spin-polarization vector parallel to the photon spin) and ξ (characterizing the component $P_\perp$ perpendicular to the reaction plane) of the photoelectrons for the two ionic fine-structure components $HI^+ \, ^2\Pi_{3/2}$ (v = 0) and $^2\Pi_{1/2}$ (v = 0) were determined in the wavelength range of 120 nm to 60 nm using the Mott detector. In addition, the spin polarization asymmetry parameter α was obtained from a measurement of the angular dependence of $A(\theta)$ at $\lambda = 100$ nm. The measurement procedure utilizing the reaction geometry of the experiment is described in Ref. 6.

In comparison to its united atom, xenon, the symmetry is reduced for hydrogen iodide due to the nonspherical molecular potential and the highest degree of photoelectron-spin polarization attainable is 50% since all possible orientations of the molecular axis with respect to the photon momentum have to be averaged[12]. In the nonrelativistic theory the influence of the spin-orbit interaction on the continuous spectrum is neglected and the relationships

$$(1)\ A_{3/2} = -A_{1/2} \qquad (2)\ \xi_{3/2} = -\xi_{1/2} \qquad (3)\ \alpha_{3/2} = -\alpha_{1/2}$$

at equal photoelectron energy hold.[12,13]

The experimental results for A and ξ are shown in Figs. 6 and 7, respectively. Also drawn (full curves) are recent nonrelativistic ab-initio calculations (frozen-core static exchange approximation) of Raseev et al.[13]. A comparison of theory and experiment is more favorable for the spin-polarization parameter A than for ξ. Although smaller in absolute value, the experimental data for the A parameter have the same shape of the wavelength dependence as the calculated values. Comparing equal photoelectron energy, the relation (1) is fulfilled approximately for A, but equation (2) for ξ does not hold for the experimental values and the disagreement between experiment and theory is larger. Similar deviations were noted before in experiments with molecules containing heavy halogen atoms[14]. Since ξ is determined from off-diagonal interference terms in the theory and its dynamical factor depends on the sine of phase-shift differences of continuum wavefunctions it is more sensitive to the influence of the spin-orbit interaction in the continuum than the other dynamical parameters in molecular photoionization. (The parameter A is independent of phase-shift differences and the asymmetry parameters β and α have a different phase dependence and are dominated by diagonal terms.)

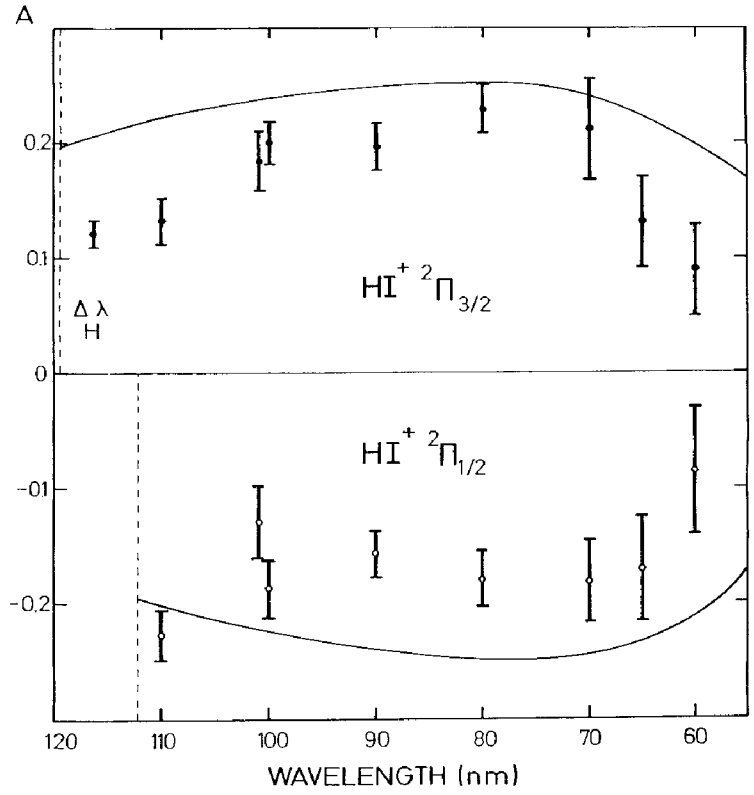

Fig. 6: Spin-polarization parameter A for $HI^+ {}^2\Pi$ (v = 0).
Data points: this work, full curves: calculation of Ref. 13.

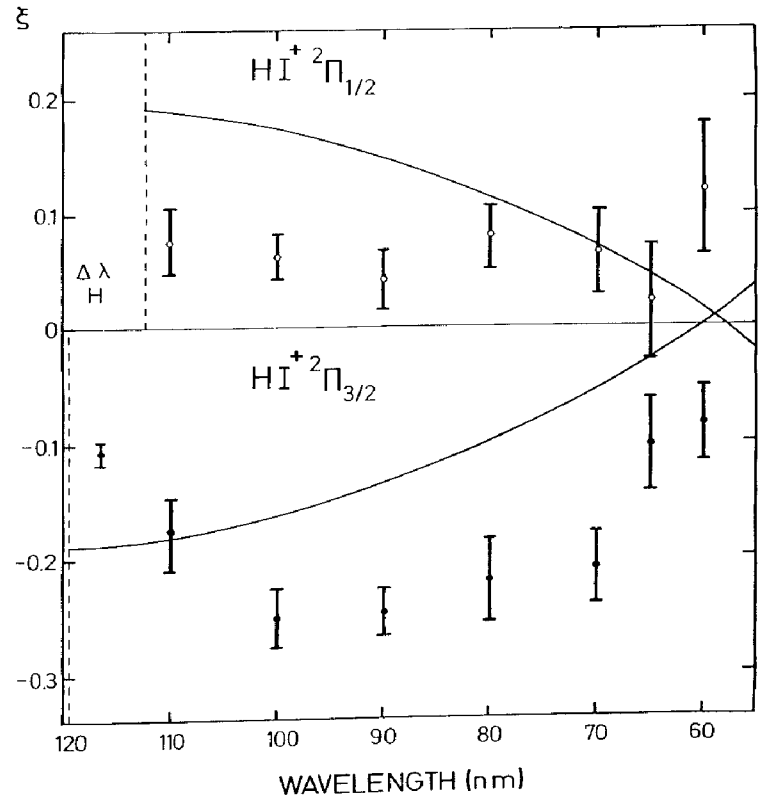

Fig. 7: Spin-polarization parameter ξ for $HI^+ {}^2\Pi$ (v = 0).
Data points: this work, full curves: calculation of Ref. 13.

From a least-squares fit of the angular distributions measured for $A(\theta)$ at λ = 100 nm, we have obtained $\alpha_{3/2}$ = 0.31±0.03 and $\alpha_{1/2}$ = -0.19±0.02, to be compared with $\alpha_{3/2}$ = 0.39, $\alpha_{1/2}$ = -0.41 of Raseev et al.[13].

CONCLUSION

Hydrogen iodide has proven to be very suitable to probe the extent and influence of vibrational and rotational structure in the autoionization spectra as well as the spin polarization of the photoelectrons. Furthermore, theoretical calculations are available[5,13] for comparison with the experimental results. Using circularly polarized light, substantial photoelectron-spin polarization was found for the $^2\Pi$ fine-structure components and the energy dependence of the corresponding parameters was examined. The vibrationally resolved measurements have demonstrated that photoelectron spectroscopy with a tunable light source can reveal vibrational excitation which, due to predissociation, is not spectroscopically accessible in photoabsorption experiments. Finally, using laser-frequency upconversion, resolving powers exceeding 2×10^5 can be achieved in the VUV with sufficient intensities for photoelectron emission experiments probing rotational structures in photoionization.

ACKNOWLEDGEMENT

Financial support by the Bundesministerium für Forschung und Technologie (05331AXIO) and the Deutsche Forschungsgemeinschaft (Sfb 216) is gratefully acknowledged.

REFERENCES

1. T. Huth, A. Mank, N. Böwering, G. Schönhense, R. Wallenstein and U. Heinzmann, to be published.
2. N. Böwering, M. Müller and U. Heinzmann, to be published.
3. R. Hilbig and R. Wallenstein, IEEE J. Quantum Electron. 19:1759 (1983).
4. J. H. D. Eland and J. Berkowitz, J. Chem. Phys. 67:5034 (1977).
5. H. Lefebvre-Brion, A. Giusti-Suzor and G. Raseev, J. Chem. Phys. 83:1557 (1985).
6. Ch. Heckenkamp, F. Schäfers, G. Schönhense and U. Heinzmann, Z. Phys. D 2:257 (1986).
7. D. W. Turner, C. Baker, A. D. Baker and C. R. Brundle, in: "Molecular Photoelectron Spectroscopy", p. 59, Wiley, New York (1972).
8. H. J. Lempka, T. R. Passmore and W. C. Price, Proc. Roy. Soc. A 304:53 (1968).
9. T. A. Carlson, P. Gerard, M. O. Krause, G. Von Wald, J. W. Taylor and F. A. Grimm, J. Chem. Phys. 84:4755 (1986).
10. D. T. Terwilliger and A. L. Smith, J. Chem. Phys. 63:1008 (1975).
11. P. M. Dehmer and W. A. Chupka, Argonne National Laboratory Report ANL-78-65, Part I:p. 13 (1978).
12. N. A. Cherepkov, J. Phys. B 14:2165 (1981).
13. G. Raseev, F. Keller and H. Lefebvre-Brion, Phys. Rev. A, to be published, and private communication.
14. G. Schönhense, V. Dzidzonou, S. Kaesdorf and U. Heinzmann, Phys. Rev. Lett. 52:811 (1984).